



# Radiation synthesis and anticancer drug delivery of poly(acrylic acid/acrylamide) magnetite hydrogel

Nasser Mohammed Hosny<sup>1</sup> · Mohammed Abbass<sup>1</sup> · Faten Ismail<sup>2</sup> · Horia M. Nizam El-Din<sup>2</sup>

Received: 7 February 2022 / Revised: 3 May 2022 / Accepted: 11 May 2022 /

Published online: 29 May 2022

© The Author(s) 2022

## Abstract

Hydrogels had gained considerable importance in drug delivery systems. Polyacrylic acid/acrylamide (AAc/AAM) and polyacrylic acid/acrylamide doped with magnetite (AAc/AAM)Fe<sub>3</sub>O<sub>4</sub> hydrogels have been prepared by  $\gamma$ -radiations and characterized by Fourier transform infrared spectra (IR), X-ray diffractions (XRD), scanning electron microscope (SEM) and transmittance electron microscope (TEM). The morphology and the particle size were determined from TEM images. The average particle size of Fe<sub>3</sub>O<sub>4</sub> was found to be 12 nm. The degree of cross-linking of Poly (AAc/AAM) hydrogel was determined from the gel fraction at different radiation doses and compositions. Swelling of the hydrogel was studied at different conditions. The magnetism of (AAc/AAM) Fe<sub>3</sub>O<sub>4</sub> was studied by vibrating sample magnetometer and the results indicated super-paramagnetic character of (AAc/AAM)Fe<sub>3</sub>O<sub>4</sub>. The band gap ( $E_g$ ) was determined and the values suggested semi-conductivity of the hydrogels. Doxorubicin loading and release by (AAc/AAM)Fe<sub>3</sub>O<sub>4</sub> hydrogel was studied and indicated that the hydrogel can load 78% of doxorubicin.

**Keywords** Polyacrylic acid/acrylamide · Radiation synthesis · Swelling · Doxorubicin · Drug delivery

---

✉ Nasser Mohammed Hosny  
Nasserh56@yahoo.com

<sup>1</sup> Chemistry Department, Faculty of Science, Port Said University, P.O. BOX 42522, Port Said, Egypt

<sup>2</sup> Polymer Chemistry Department, National Center for Radiation Research and Technology, Cairo, Egypt

## Introduction

Hydrophilic gels are an important category of cross-linked polymers that absorb water without dissolution. Hydrogels have interesting properties as softness, smart and ability to store water [1].

The polymers that can change their properties by changing the chemical or physical stimuli, are known as “smart” polymers. Hydrogels are sensitive to the change in the surrounding environmental conditions due to the presence of various functional groups along the polymer chains. Poly acrylic acid is affected by the change in the pH of the medium, so it has wide applications in the drug delivery to the gastrointestinal tract [2]. Hydrogels are soft materials that have wide biological applications for half a century. They have good biocompatible advantages which come from their higher swelling ability. On the contrary, they exhibit some limitations to mechanical properties and consequently the applications. The effects of starting materials, fabrication factors as mechanical stress and swelling have been studied [3].

The unique properties of metal oxide nanoparticles are associated with its surface area [4–7]. The application of hydrogel in drug delivery, biosensors and tissue engineering was recently reviewed [8]. The role of hydrogel in transdermal drug delivery was also reviewed [9]. In addition to that, the rheological behavior was extensively studied by Hsissou et al. [10–14]

Delivery of water soluble or insoluble pharmaceuticals is a key challenge in nanomedicine. Polymer hydrogels had gained considerable importance in drug delivery systems. Hydrogels have several advantages as they are easily synthesized, elastic, soft and environmentally safe materials which make them suitable for nanomedical applications [15].

In this manuscript, the synthesis, spectral, swelling, magnetic and drug release properties of polyacrylic acid/acrylamide, magnetite hydrogel have been studied to shed some light on the potential medical applications of these hydrogels.

Previously, acrylic acid/ acrylamide was prepared by potassium persulfate as an initiator and N,N'-methylene bisacryl-amide as a cross-linking agent [16]. The present work has some advantages as it used radiation in synthesis and as a cross-linking agent. In addition to that, the obtained composites have higher swelling ability and could be applied as a carrier of the well-known anticancer drug Doxorubicin.

## Experimental

Acrylic acid, 99%, Acrylamide, 99%,  $\text{FeSO}_4 \cdot 7\text{H}_2\text{O}$ , 99% and  $\text{FeCl}_3 \cdot 6\text{H}_2\text{O}$ , 99% were purchased from Sigma-Aldrich.

### Preparation of acrylic acid (AAc)/acrylamide (AAM) by gamma radiations

Stock solutions of AAc and AAm were prepared as follows: 20 mL of acrylic acid in 100 ml distilled water; 5 mL of acrylamide was dissolved in 100 ml distilled water.

From the stocks the following ratios of AAc/AAM (10/90, 30/70, 50/5, 70/30 and 90/10) were prepared. Nitrogen gas was passed in the mixture for 5 min and then subjected to gamma radiation.

The source of radiation is  $^{60}\text{Co}$  gamma cell and the dose rate was 5 KGy/h.

### Preparation of acrylic acid, acrylamide, magnetite (AAc/AAM) $\text{Fe}_3\text{O}_4$

$\text{FeSO}_4 \cdot 7\text{H}_2\text{O}$  and  $\text{FeCl}_3 \cdot 6\text{H}_2\text{O}$  were mixed in 1:2 ratio in 100 mL distilled water. Let the mixture overnight. To the above mixture AAc/AAM in different ratios were added. Then, 1 M ammonium hydroxide was added drop by drop until black color appears then irradiated with different doses of gamma radiations with dose rate 5 KGy/hr.

### Swelling study

Swelling of AAc/AAM was carried out as follows: A dry weight of the hydrogel ( $W_1$ ) was immersed in distilled  $\text{H}_2\text{O}$  at room temperature for various time intervals. Then remove excess of water by a filter paper and reweigh ( $W_2$ ). The % of swelling ( $S$ ) was found from the relation  $S = (W_2 - W_1/W_1) \times 100$ .

### Gel fraction determination

A weighed sample ( $W_1$ ) of the polymer was boiled in  $\text{H}_2\text{O}$  (distilled) for 4 h and dry in a vacuum oven at 80 °C, till constant weight ( $W_2$ ). The gel fraction% ( $F$ ) was calculated:  $F = (W_2/W_1) \times 100$ .

### Doxorubicin loading

0.1 g of AAM/AAc/ $\text{Fe}_3\text{O}_4$  nanocomposite was immersed in 2 mL of 0.5 mM of Doxorubicin in distilled water for 24 h. Finally, the polymer was washed by distilled water then, dried at 50 °C. The drug loaded was studied at pH 5.0, 7.4 and 8.0 for 24 h. The loaded amount of the drug was determined using UV–vis spectrophotometer at 470 nm.

### Drug release measurements

Doxorubicin release were followed at 37 °C for approximately 24 h. Release experiments were done by placing various nanocomposite samples loaded with drug (conc. 0.5 mM) into 30 mL buffer solutions of pH 5, 7.4, 8. A sample was taken and measured at 470 nm at different time intervals.

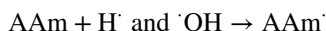
The amount of drug released from nanocomposite hydrogel was calculated using the equation: Drug release (%) =  $\left[ \frac{\text{amount of drug released}}{\text{amount of drug loaded}} \times 100 \right]$ .

### Working procedures

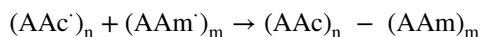
Infrared spectra (FT-IR): The prepared hydrogels were measured using (FT-IR-4100 type A) at Damietta University. Electronic spectra (UV–Vis) of the isolated compounds were recorded on (Hach Model DR-6000) at Egyptian propylene and poly propylene company. X-ray powder diffraction patterns were taken on Philips X'PERT-PRO diffract meter, with wavelength is 1.5406 Å. Transmission electron microscope images of hydrogels were taken on transmission electron microscope (JEOL JEM-2100) at Egyptian petroleum research institute (EPRI), Cairo.

### Results and discussion

Polyacrylic acid/acrylamide (AAc/AAm) hydrogel was synthesized by gamma irradiation in aqueous solution. The cross-linking of poly (AAc/AAm) in aqueous media was mediated by radiation. The suggested mechanism of cross-linking is as follow: The solvent (HOH) and the monomers (AAc and AAm) absorb gamma radiation forming activated compounds (AAc\*, AAm\* HOH\*). Then, the activated compounds can undergo fragmentations forming free radicals of AAc·, AAm·, H· and ·OH. The radicals of the solvents can transfer to AAc and AAm forming more of these radicals and increasing the rate of cross-linking [17, 18].



In the termination, step (*n*) or (*m*) repeating units combine to form cross-linked polymers



### Encapsulation of magnetite in P(AAc/AAm) hydrogel matrix

XRD pattern of magnetite doped (Fig. 1) shows the peaks at  $2\theta = 30.2, 35.7, 43.0, 57.0$  and  $63.0^\circ$  attributed to the planes (220), (311), (400), (422) and (440), respectively. These planes confirm that the sample is  $\text{Fe}_3\text{O}_4$  with face centered cubic structure (JCPDS) 19-0629. The broadening of the peaks is attributed to the presence of the particles in the nanoscale.

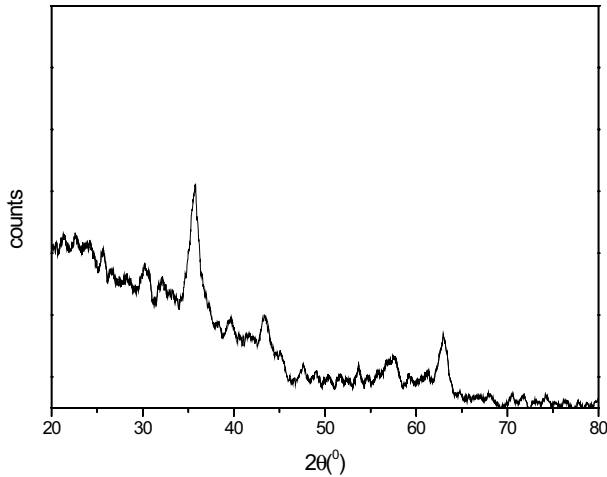


**Fig. 1** XRD pattern of Poly (AAc/AAm)Fe<sub>3</sub>O<sub>4</sub>

Debye–Scherer equation  $D=0.94\lambda/\beta \cos\theta$  [19] ( $D$  is the crystallite size,  $\lambda=1.5406 \text{ \AA}$ ,  $\beta$  is the width at half maximum) was applied to determine the crystallite size from the peak at  $35.7^\circ$  and it was 12 nm.

One of the most characteristic features of the hydrogel is its high ability to uptake water. So, magnetite was doped from aqueous media in the hydrogel matrix by in situ procedures.

TEM image of Poly (AAc-co-AAm) Fe<sub>3</sub>O<sub>4</sub> hydrogel is indicated in Fig. 2A.

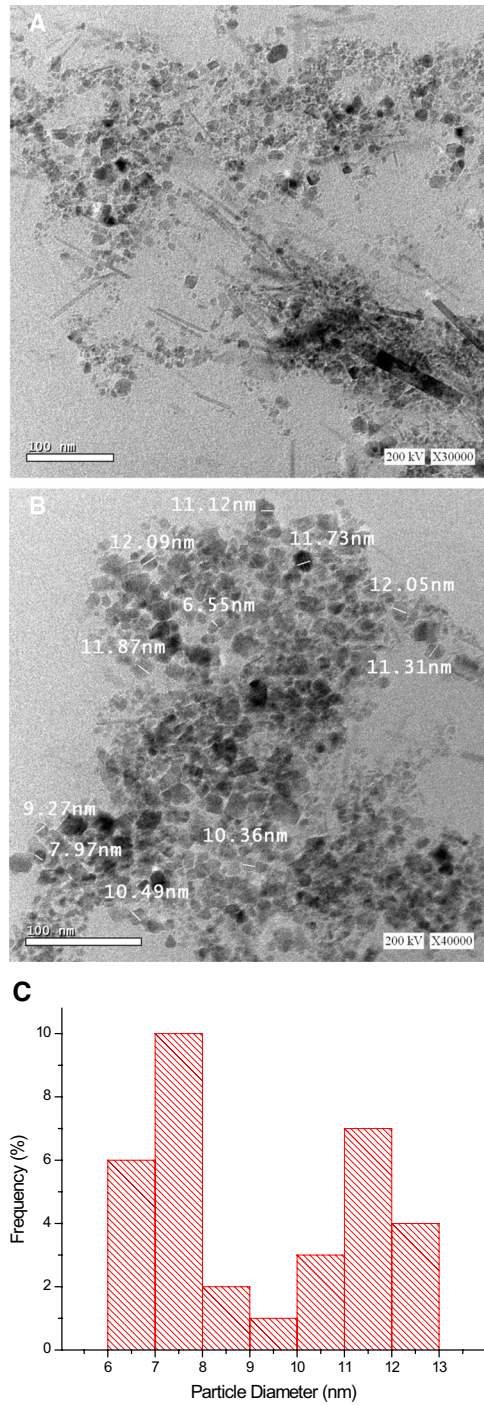
The high contrast in TEM images was used to confirm encapsulation of Fe<sub>3</sub>O<sub>4</sub> nanoparticles in P(AAc/AAm) hydrogel matrix. As indicated from TEM analysis, the black spheres point to magnetite nanoparticles that encapsulated inside the hydrogel core and they are not outside the hydrogel. It is clear (Fig. 2B) that some magnetite nanoparticles aggregated to form rods. The particle size distribution curve of magnetite encapsulated in P(AAc/AAm) (Fig. 2C) indicates the distribution of the particle in small range from 6 to 13 nm with two maxima at 7.5 and 11.5 nm.

## FT-IR spectra

IR of Poly(AAc/AAm) Fe<sub>3</sub>O<sub>4</sub> spectrum (Fig. 3) reveals a band at  $568 \text{ cm}^{-1}$  characteristic to  $\nu(\text{Fe-O})$  in octahedral site of Fe<sub>3</sub>O<sub>4</sub>. The bands at  $637$  and  $609 \text{ cm}^{-1}$  are characteristic also to Fe–O bonds in magnetite [3].

The stretching vibrations of  $\nu(\text{OH})$  of acrylic acid appear at  $3412 \text{ cm}^{-1}$  [3]. The bands at  $3337 \text{ cm}^{-1}$  and  $3189 \text{ cm}^{-1}$  are due to  $\nu_{\text{as}}$  and  $\nu_{\text{s}}$  of NH<sub>2</sub> of acrylamide [3]. The absence of the bands assigned to (CH<sub>2</sub>=CH–) in both AAc and AAm confirms the polymerization of AAc and AAm through this group. In the

**Fig. 2** TEM images of (AAc/AAm) $\text{Fe}_3\text{O}_4$ . **C** Particle size distribution of  $\text{Fe}_3\text{O}_4$  encapsulated in Poly(AAc/AAm)



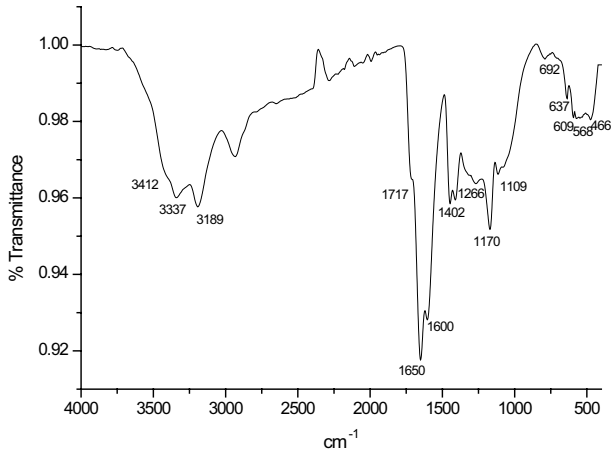


**Fig. 3** IR spectrum of Poly (AAc/AAm)  $\text{Fe}_3\text{O}_4$

spectrum of Poly(AAc/AAm)  $\text{Fe}_3\text{O}_4$ , the positions of the bands at 1617 and  $1650\text{ cm}^{-1}$ , which were attributed to protonated (COOH) group [20] and  $\nu_5$  (CO) of acrylamide did not change compared with their positions in the free polymer, while there are shifts to lower wavenumber in the bands  $1607$  and  $1402\text{ cm}^{-1}$  that were attributed to  $\nu_{\text{as}}$  and  $\nu_{\text{s}}$  (COOH). These shifts suggest the possibility of electrostatic attraction between  $\text{Fe}_3\text{O}_4$  and this group.

### Gel fraction

To determine the degree of cross-linking of Poly (AAc/AAm) hydrogel, the gel fraction was calculated at different radiation doses and compositions (Fig. 4A). The gel fraction was calculated by applying the relation.

$\text{Gel (\%)} = W_d/W_i \times 100$  (where  $W_d$  is the weight of extracted hydrogel and  $W_i$  is the weight of dry hydrogel).

From the curves, it is clear that the degree of cross-linking increases with increase of the radiation dose. At composition ratio AAC:AAM (30:70), the hydrogels have approximately the same gel fraction % regardless of the applied radiation doses. The hydrogel synthesized at radiation dose 50 KGy exhibits the maximum cross-linking at composition ratio 50:50 (AAC:AAM); then, the cross-linking decreases with increasing composition ratios. The cross-linking of the hydrogels synthesized by radiation doses 10 and 30 KGy begins to decrease after composition ratios (30:70) AAC:AAM. In the beginning when aqueous solution of AAC/AAM was subjected to radiation, free radicals of AAC, AAM and water will generate and they can combine randomly forming cross-link of co and homo-polymer AAC. When two radicals of neighboring polymeric chains combine a cross-linked macromolecules will be formed. As the concentration and radiation dose increase the presence of higher number of the rigid cross-linked polymer with

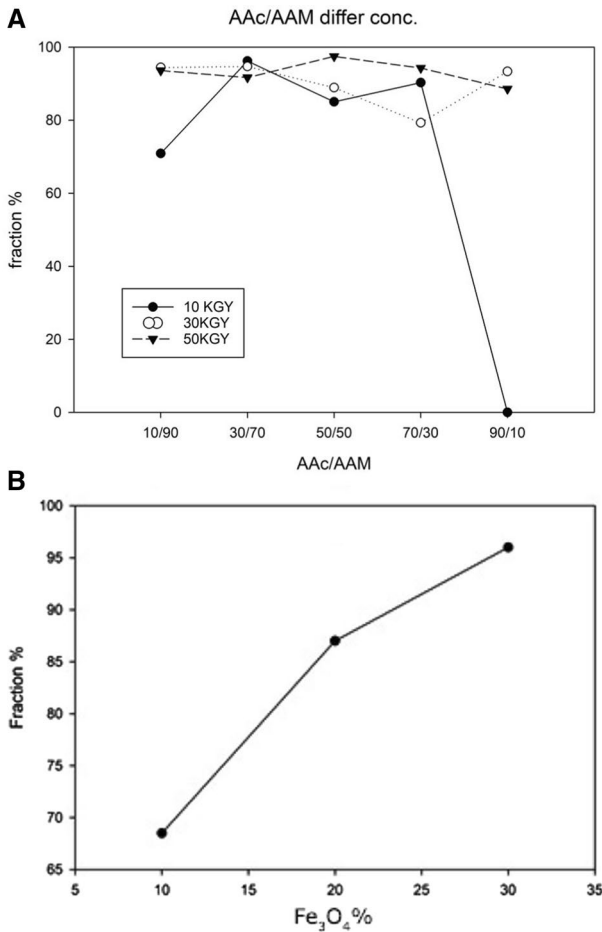


**Fig. 4** Gel fraction at (A) different radiation dose and composition of AAc/AAM and different concentration of magnetite at composition 10/90 AAc/AAM and 30 KGy (B)

low mobility will increase. In the same time, the possibility of formation of more cross-linked polymer will decrease [21].

From Fig. 4B, it is clear that the gel fraction percentage increases as the concentration of magnetite increases as  $Fe^{2+}$  and  $Fe^{3+}$  in magnetite can bind neighbor polymeric chains together through coordination with the active donor sites in the polymers.

## Swelling

Hydrogels exist in three-dimensional (3D) networks with hydrophilic character. They have excellent capacity of water swelling through bonding the water molecules



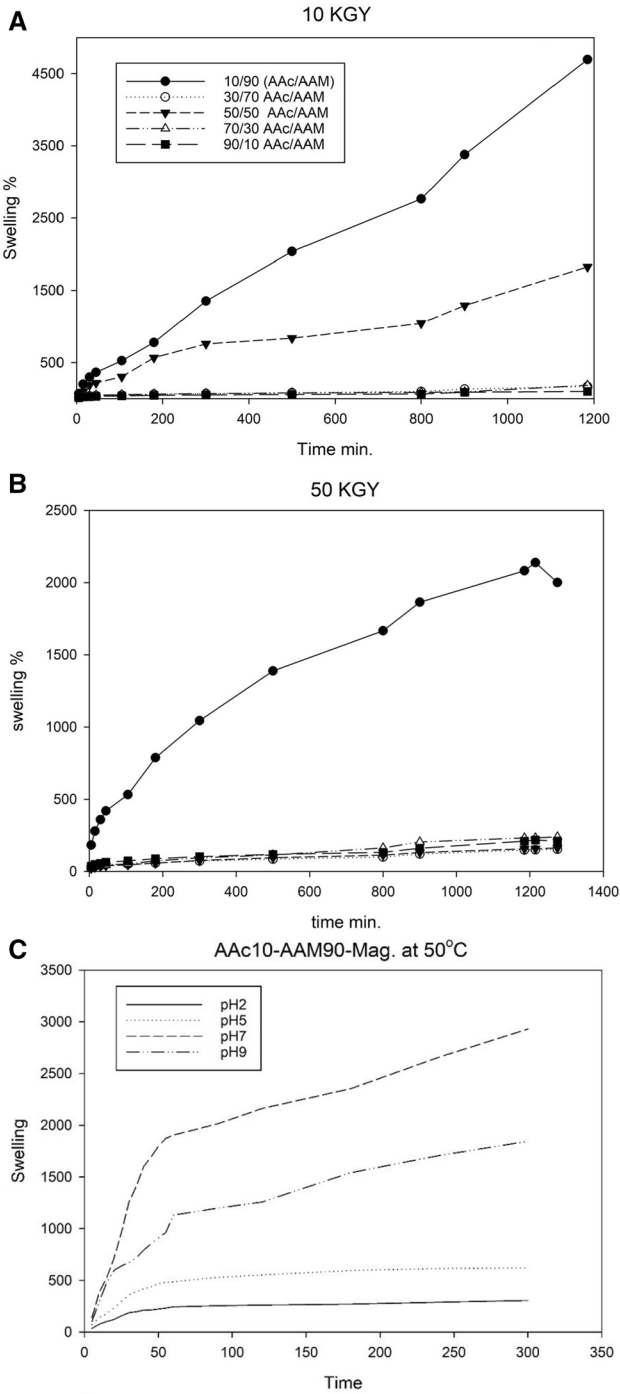


**Fig. 5** Effect of Ac composition, radiation dose and pH on swelling of (AAc/AAM) hydrogel

by the polar hydrophilic groups or by occlusion the water molecules in the gaps between the chains [22]. The effect of radiation doses from (10 to 50 KGy) on the swelling of (AAc/AAm) showed that the highest swelling value of the hydrogel is observed at the lower radiation dose 10 KGy (Fig. 5A). There is a decrease in swelling at higher dose (50 KGy) (Fig. 5B). This behavior can be interpreted on the basis of increasing the cross-linking associated with decreasing the swelling [23]. It is noticeable that, with increasing cross-linking density, there is a decrease in the separating space between the chains leading to rigidity of the formed polymer. The rigid copolymer structure will resist expansion and holding large quantities of water [24, 25].

The swelling increases also, as the concentration of AAc increases. The increment in swelling values at lower concentration is attributed to the higher hydrophilicity of the hydrogel. Then, the decrease in swelling with concentration could be resulted from the increased chance of terminating AAc radicals. In addition, the viscosity of the reaction increases at higher AAc concentration, which restricts the mobility of the monomeric radicals and deactivates grow of the polymeric chains. It can be suggested also that there will be an enhancement in homo-polymerization reaction over copolymerization [26–28].

With respect to the increase in the swelling, the pH increases (Fig. 5C). It is noticeable that at higher pH the alkaline medium will affect on the hydrophilic groups as hydroxyl, carboxyle and amide of the reactants leading to increase the possibility of hydrogen bonding and consequently, increasing the swelling.

The swelling of hydrogels was studied in the temperature range (30–70 °C). The results indicated that, by raising temperature, the swelling % increases until 50 °C, then the swelling % decreases by raising temperature. In the first stage raising temperature may increase the mobility of the polymers and activate them to absorb water molecules, at higher temperature there will be breaking in hydrogen bond and liberation of water molecules.

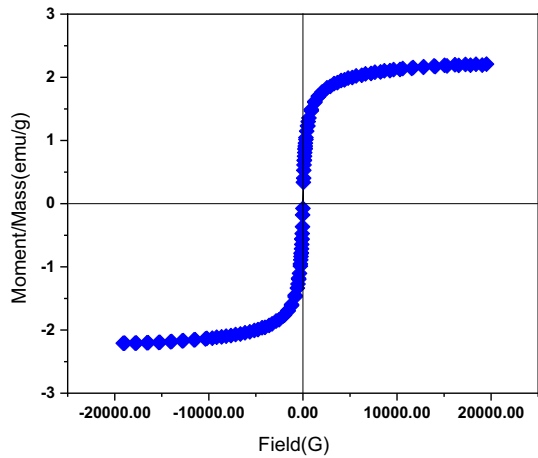
## Magnetic properties

The super-paramagnetism of  $\text{Fe}_3\text{O}_4$  nanoparticles is important for their application in therapeutic applications. Super-paramagnetic nanoparticles have magnetism in the presence of external magnetic field and lose it in the absence of the field. If there is no hysteresis, both the retentivity ( $M_r$ ) and coercivity ( $H_c$ ) are zero or very close to zero, the material is characterized as super-paramagnetic.

The critical size of super-paramagnetic material is ca. 20 nm for soft magnets and 4 nm for hard ones [29]. Also, there is a direct relation between saturation magnetization of the nanoparticles and the size. By decreasing the particle size, the magnetization will be lowered. When the size of magnetite is reduced to the nanoscale, they exhibit super-paramagnetism [30, 31].

The magnetism of (AAc/AAm)  $\text{Fe}_3\text{O}_4$  was studied by vibrating sample magnetometer at 25 °C (Fig. 6). The curve shows no hysteresis and the saturation magnetization ( $M_s$ ) is 2.2 emu/g due to the presence of  $\text{Fe}_3\text{O}_4$  in nanoscale and

**Fig. 6** VSM of (AAc/AAm) Fe<sub>3</sub>O<sub>4</sub> hydrogel



the effect of diamagnetic polymers. Both retentivity ( $M_r$ ) and coercivity ( $H_c$ ) are  $48 \times 10^{-3}$  emu/g and 7.8 G, respectively, which are close to zero. From these findings it could be concluded that Fe<sub>3</sub>O<sub>4</sub> (AAc/AAm) is a super-paramagnetic material.

### Optical band gap ( $E_g$ )

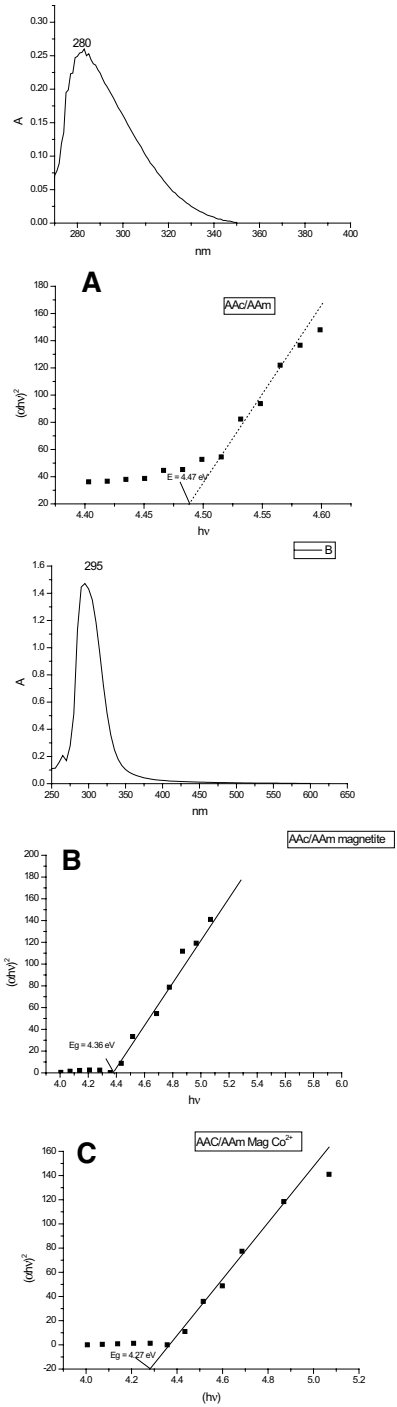
Electronic absorption spectrum of poly (AAc/AAm) shows an absorption band centered at 280 nm due to  $n-\pi^*$  transitions. This band was shifted to 295 nm in case of (AAc/AAm) Fe<sub>3</sub>O<sub>4</sub> as a result of interaction between the metal orbital with that of the polymer, forming charge transfer from organic polymer to the metal.

The spectra of hydrogels were used to determine  $E_g$  of these compounds by applying Tauc’s equation: [32]  $(\alpha h\nu)^2 = B (h\nu - E_g)^m$   $m$  is equal to 1/2 for indirect transition and 2 for direct transition. The absorption coefficient ( $\alpha$ ) is given from the relation  $\alpha = A/d$  where  $A$  = absorbance,  $d$  is the path length through the sample. The parameter ( $B$ ) represents transition probability. The graphical representation of  $(\alpha h\nu)^2$  against  $h\nu$  gives direct transitions when extrapolating the linear portion of the curve to  $(\alpha h\nu)^2 = 0$  (Fig. 7).  $E_g$  values are 4.47 and 4.36 eV for poly (AAc/AAm) and (AAc/AAm) Fe<sub>3</sub>O<sub>4</sub>, respectively. The reduction in  $E_g$  value after encapsulation Fe<sub>3</sub>O<sub>4</sub>, comes from the interaction between the polymers orbitals with that of the metal orbital forming new larger molecular orbitals. The increment in the orbital leads to reduction of  $E_g$ . The values of  $E_g$  indicate that these hydrogels are semi-conductors [33, 34].

### Release of doxorubicin

Doxorubicin is a well-known anticancer chemotherapy drug. Doxorubicin belongs to anthracycline antibiotic.

**Fig. 7** Optical band gap of **A** (AAc/AAm) and **B** (AAc/AAm)  $\text{Fe}_3\text{O}_4$



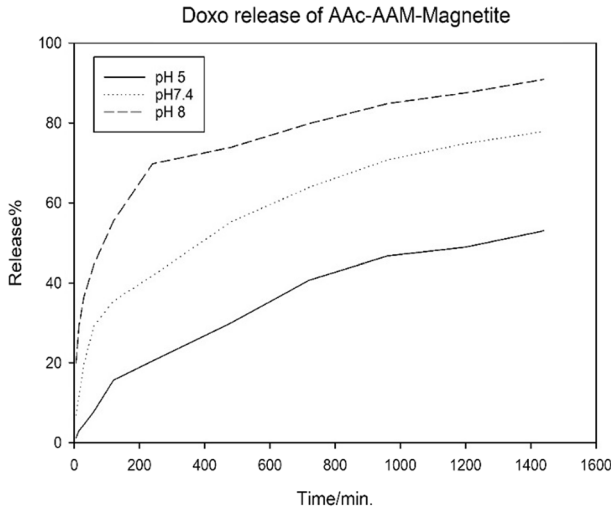


**Fig. 8** Doxorubicin release profile of (AAc/AAM) Fe<sub>3</sub>O<sub>4</sub>

The drug-loading % of hydrogel was calculated using the following relation:

$$\text{Loading of drug \%} = \frac{\text{Weight of drug in hydrogel/}}{\text{Weight of hydrogel loaded with drug}} \times 100$$

The drug loading percent was found to be 78.0%

The release profile of doxorubicin from (AAc/AAM)Fe<sub>3</sub>O<sub>4</sub> at pH's 5, 7.4 and 8 has been studied (Fig. 8). The release is high in the beginning at the three pH, then it becomes slow at equilibrium. The release rate increases as pH increases, the slowest release is observed in the acid medium, while the release is high in the basic medium. This can be explained based on adsorption of Doxorubicin onto AAc/AAM magnetite hydrogel either through coordination of doxorubicin hydroxyl groups with magnetite or through formation of hydrogen bonds with COOH and amide group of AAc/AAM.

At high pH, there is a competition between the hydroxyl group of medium and that of Doxorubicin, so, the rate of release increases [35, 36].

## Conclusion

Polyacrylic acid/acrylamide (AAc/AAM) and polyacrylic acid/acrylamide magnetite (AAc/AAM)Fe<sub>3</sub>O<sub>4</sub> hydrogels have been synthesized and tested for loading and release of the anticancer drug Doxorubicin. Swelling study was carried out to determine the suitable conditions for swelling the hydrogel. The optical band gap was determined for the two polymers and indicated semi-conducting nature of the two polymers. (AAc/AAM)Fe<sub>3</sub>O<sub>4</sub> hydrogel can load 78% of Doxorubicin and release

it in the alkaline medium. (AAc/AAm)Fe<sub>3</sub>O<sub>4</sub> hydrogel is a potential candidate for chemotherapy anticancer drugs delivery.

**Funding** Open access funding provided by The Science, Technology & Innovation Funding Authority (STDF) in cooperation with The Egyptian Knowledge Bank (EKB).

## Declarations

**Conflict of interest** The authors declare that they have no conflict of interest.

**Open Access** This article is licensed under a Creative Commons Attribution 4.0 International License, which permits use, sharing, adaptation, distribution and reproduction in any medium or format, as long as you give appropriate credit to the original author(s) and the source, provide a link to the Creative Commons licence, and indicate if changes were made. The images or other third party material in this article are included in the article's Creative Commons licence, unless indicated otherwise in a credit line to the material. If material is not included in the article's Creative Commons licence and your intended use is not permitted by statutory regulation or exceeds the permitted use, you will need to obtain permission directly from the copyright holder. To view a copy of this licence, visit <http://creativecommons.org/licenses/by/4.0/>.

## References

1. Gerlach G, Arndt KF (2009) Hydrogel sensors and actuators, Springer series on chemical sensors and biosensors, 6th edn. Springer-Verlag, Berlin Heidelberg
2. Nesrinne S, Djamel A (2017) Synthesis, characterization and rheological behavior of pH sensitive poly(acrylamide-co-acrylic acid) hydrogels. Arab J Chem 10:539–547. <https://doi.org/10.1016/j.arabjc.2013.11.027>
3. Stoia M, Istrate R, Păcurariu C (2016) Investigation of magnetite nanoparticles stability in air by thermal analysis and FTIR spectroscopy. J Therm Anal Calorim 125:1185–1198. <https://doi.org/10.1007/s10973-016-5393-y>
4. Hosny NM, Sherif YE (2022) Synthesis, optical band gap and anti-rheumatic activity of Fe<sub>2</sub>O<sub>3</sub> nanocrystals via solid state decomposition of 4-aminophenol precursor. Chem Data Collect 37:100813. <https://doi.org/10.1016/j.cdc.2021.100813>
5. Hosny NM (2014) Single crystalline Co<sub>3</sub>O<sub>4</sub>: synthesis and optical properties. Mater Chem Phys 144:247–251. <https://doi.org/10.1016/j.matchemphys.2013.12.022>
6. Hosny NM, Dahshan A (2012) Facile synthesis and optical band gap calculation of Mn<sub>3</sub>O<sub>4</sub> nanoparticles. Mater Chem Phys 137:637–643. <https://doi.org/10.1016/j.matchemphys.2012.09.068>
7. Hosny NM (2011) Synthesis, characterization and optical band gap of NiO nanoparticles derived from anthranilic acid precursors via thermal decomposition route. Polyhedron 30:470–476. <https://doi.org/10.1016/j.poly.2010.11.020>
8. Wang K, Hao Y, Wang Y, Chen J, Mao L, Deng Y, Chen J, Yuan S, Zhang T, Ren J, Liao W (2019) Functional hydrogels and their application in drug delivery, biosensors, and tissue engineering. Int J Polym Sci. <https://doi.org/10.1155/2019/3160732>
9. Ahsan A, Tian WX, Farooq MA, Khan DH (2021) Overview of hydrogels and their role in transdermal drug delivery. Int J Polym Mater Polym Biomater 70:574–584. <https://doi.org/10.1080/00914037.2020.1740989>
10. Hsissou R, Seghiri R, Benzekri Z, Hilali M, Rafik M, Elharfi A (2021) Polymer composite materials: a comprehensive review. Compos Struct 262:113640. <https://doi.org/10.1016/j.compstruct.2021.113640>
11. Hsissou R, Bekhta A, Dagdag O, El Bachiri A, Rafik M, Elharfi A (2020) Rheological properties of composite polymers and hybrid nanocomposites. Heliyon. <https://doi.org/10.1016/j.heliyon.2020.e04187>

12. Hsissou R, Dagdag O, Berradi M, El Bouchti M, Assouag M, El Bachiri A, Elharfi A (2019) Investigation of structure and rheological behavior of a new epoxy polymer pentaglycidyl ether pentabishphenol A of phosphorus and of its composite with natural phosphate. *SN Appl Sci* 1:869. <https://doi.org/10.1007/s42452-019-0911-8>
13. Hsissou R, Berradi M, El Bouchti M et al (2019) Synthesis characterization rheological and morphological study of a new epoxy resin pentaglycidyl ether pentaphenoxy of phosphorus and their composite (PGEPPP/MDA/PN). *Polym Bull* 76:4859–4878. <https://doi.org/10.1007/s00289-018-2639-9>
14. Hsissou R, El Bouchti M, El Harfi A (2017) Elaboration and Viscosimetric Viscoelastic and Rheological studies of a new hexafunctional polyepoxide polymer: hexaglycidyl ethylene of methylene dianiline. *J Mater Environ Sci* 8:4349–4361
15. Gonçalves C, Pereina P, Gama M (2010) Self-assembled hydrogel nanoparticles for drug delivery applications. *Materials* 3:1420–1460. <https://doi.org/10.3390/ma3021420>
16. Chenga W, Hua X, Zhao Y, Wu M, Hu Z, Yu X (2017) Preparation and swelling properties of poly(acrylic acid-co-acrylamide) composite hydrogels. *E-Polymers* 17:95–106
17. Umemura J, Hayashi S (1974) Infrared spectra and molecular configurations of liquid and crystalline acrylic acids. *Bull Inst Chem Res Kyoto Univ* 52:585–595
18. Durmazm S, Okay O (2000) Acrylamide/2-acrylamido-2-methylpropane sulfonic acid sodium salt-based hydrogels: synthesis and characterization. *Polymer* 41:3693–3704. [https://doi.org/10.1016/S0032-3861\(99\)00558-3](https://doi.org/10.1016/S0032-3861(99)00558-3)
19. Klug H, Alexander L (1974) X-ray diffraction procedures: for polycrystalline and amorphous materials, 2nd edn. Wiley, New York
20. Hosny NM, El Dossoki FI (2008) Schiff base complexes derived from 2-acetylpyridine, leucine, and some metal chlorides: their preparation, characterization, and physical properties. *J Chem Eng Data* 53:2567–2572. <https://doi.org/10.1021/je800415n>
21. Bhuiyan MAQ, Sh RM, Shajahan M, Dafader NC (2015) Improvement of swelling behaviour of poly (Vinyl Pyrrolidone) and acrylic acid blend hydrogel prepared by the application of gamma radiation. *Org Chem Curr Res* 4:1000138. <https://doi.org/10.4172/2161-0401>
22. Ganji F, Vasheghani-Farahani S, Vasheghani-Farahani E (2010) Theoretical description of hydrogel swelling: a review. *Iran Polym J* 19:375
23. Peppas LB, Harland RS (1990) Absorbent polymer technology. Elsevier, Amsterdam
24. Peppas NA, Mikes AG (1986) Hydrogels in medicine and pharmacy, vol 1. CRC Press, Boca Raton
25. Flory PJ (1953) Principles of polymer chemistry. Cornell University Press, Ithaca
26. Lee WF, Lin GH (1999) Superabsorbent polymeric materials. VIII. Swelling behavior of crosslinked poly[sodium acrylate-cotrimethylmethacryloyloxyethyl ammonium iodine] in aqueous salt solutions. *J Appl Polym Sci* 72:1221–1232. [https://doi.org/10.1002/\(SICI\)1097-4628\(19970531\)64:9%3c11701::AID-APP5%3e3.0.CO;2-J](https://doi.org/10.1002/(SICI)1097-4628(19970531)64:9%3c11701::AID-APP5%3e3.0.CO;2-J)
27. Athawale VD, Lele V (1998) Graft copolymerization onto starch. II. Grafting of acrylic acid and preparation of it's hydrogels. *Carbohydr Polym* 35:21–27. [https://doi.org/10.1016/S0144-8617\(97\)00138-0](https://doi.org/10.1016/S0144-8617(97)00138-0)
28. Pourjavadi A, Sadeghi M, Hosseinzadeh H (2004) Modified carrageenan: preparation, swelling behavior, salt- and pH-sensitivity of partially hydrolyzed crosslinked carrageenan-graft-polymethacrylamide superabsorbent hydrogel. *Polym Adv Technol* 15:645. <https://doi.org/10.1002/pat.52>
29. Jeong U, Teng X, Wang Y, Yang H, Xia Y (2007) Superparamagnetic colloids: controlled synthesis and Niche applications. *Adv Mater* 19:33–60. <https://doi.org/10.1002/adma.200600674>
30. Cullity BD, Graham CD (2009) Introduction to magnetic materials, 2nd edn. IEEE Press, Piscataway, p 361
31. Wasilewski PJ (1977) Magnetic and microstructural properties of some lodestones. *Phys Earth Planet Inter* 15:349–362
32. Tauc J (1968) Optical properties and electronic structure of amorphous Ge and Si. *Mater Res Bull* 3:37–46. [https://doi.org/10.1016/0025-5408\(68\)90023-8](https://doi.org/10.1016/0025-5408(68)90023-8)
33. Hosny NM, Sherif YE (2015) Synthesis, structural, optical and anti-rheumatic activity of metal complexes derived from (E)-2-amino-N-(1-(2-aminophenyl)ethylidene)benzohydrazide (2-AAB) with Ru(III), Pd(II) and Zr(IV). *Spectrochim Acta A* 136:510–519. <https://doi.org/10.1016/j.saa.2014.09.064>
34. Hosny NM, Hussien MA, Motawa R, Belal A, Abdel-Rhman MH (2020) Synthesis, spectral, modeling, docking and cytotoxicity studies on 2-(2-aminobenzoyl)-N-ethylhydrazine-1-carbothioamide and its divalent metal complexes. *Appl Organomet* 34:e5922. <https://doi.org/10.1002/aoc.5922>

35. Hosny NM, Goma I, Abd El-Moemen A, Anwar ZM (2020) Synthesis, magnetic and adsorption of dye onto the surface of NiO nanoparticles. *J Mater Sci Mater Electron* 31:8413–8422. <https://doi.org/10.1007/s10854-020-03376-w>
36. Hosny NM, Goma I, Abd El-Moemen A, Anwar ZM (2022) Adsorption of Ponceau Xylidine dye by synthesised  $Mn_2O_3$  nanoparticles. *Int J Environ Anal Chem*. <https://doi.org/10.1080/03067319.2021.2014470>

**Publisher's Note** Springer Nature remains neutral with regard to jurisdictional claims in published maps and institutional affiliations.